

AD-A151 292

A CALORIMETRIC APPROACH FOR MEASURING EMITTANCE AND  
NORMAL SPECTRAL ABSOR. (U) AEROSPACE CORP EL SEGUNDO CA  
MATERIALS SCIENCES LAB F IZAGUIRRE ET AL. 28 JAN 85  
TR-0084A(5935-04)-3 SD-TR-84-59

1/1

UNCLASSIFIED

F/G 20/6

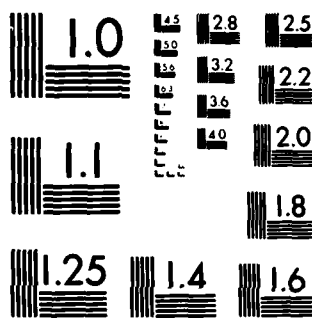
NL



END

FILED

DEC



MICROCOPY RESOLUTION TEST CHART  
NATIONAL BUREAU OF STANDARDS-1963-A

*F.*

# A Calorimetric Approach for Measuring Emittance and Normal Spectral Absorptance at Elevated Temperatures

AD-A151 292

F. IZAGUIRRE and L. FISHMAN  
Materials Sciences Laboratory  
Laboratory Operations  
The Aerospace Corporation  
El Segundo, CA 90245

28 January 1985

APPROVED FOR PUBLIC RELEASE;  
DISTRIBUTION UNLIMITED

DTIC FILE COPY

Prepared for  
SPACE DIVISION  
AIR FORCE SYSTEMS COMMAND  
Los Angeles Air Force Station  
P.O. Box 92960, Worldway Postal Center  
Los Angeles, CA 90009-2960

DTIC  
ELECTE  
MAR 18 1985

85 03 08 063

This report was submitted by The Aerospace Corporation, El Segundo, CA 90245, under Contract No. F04701-83-C-0084 with the Space Division, P.O. Box 92960, Worldway Postal Center, Los Angeles, CA 90009. It was reviewed and approved for The Aerospace Corporation by L. R. McCreight, Director, Materials Sciences Laboratory. Captain Mark D. Borchardt, SD/YNV, was the project officer for the Mission-Oriented Investigation and Experimentation (MOIE) Program.

This report has been reviewed by the Public Affairs Office (PAS) and is releasable to the National Technical Information Service (NTIS). At NTIS, it will be available to the general public, including foreign nationals.

This technical report has been reviewed and is approved for publication. Publication of this report does not constitute Air Force approval of the report's findings or conclusions. It is published only for the exchange and stimulation of ideas.

*Mark D. Borchardt*

Mark D. Borchardt, Captain, USAF  
Project Officer

*Joseph Hess*

Joseph Hess, GM-15, Director, West Coast  
Office, AF Space Technology Center

UNCLASSIFIED

SECURITY CLASSIFICATION OF THIS PAGE (When Data Entered)

REPORT DOCUMENTATION PAGE		READ INSTRUCTIONS BEFORE COMPLETING FORM
1. REPORT NUMBER SD-TR-84-59	2. GOVT ACCESSION NO. AD 1157 242	3. RECIPIENT'S CATALOG NUMBER
4. TITLE (and Subtitle) A CALORIMETRIC APPROACH FOR MEASURING EMITTANCE AND NORMAL SPECTRAL ABSORP- TANCE AT ELEVATED TEMPERATURES		5. TYPE OF REPORT & PERIOD COVERED
7. AUTHOR(s) Francisco Izaguirre and Laana Fishman		6. PERFORMING ORG. REPORT NUMBER TR-0084A(5935-04)-3
9. PERFORMING ORGANIZATION NAME AND ADDRESS The Aerospace Corporation El Segundo, Calif. 90245		8. CONTRACT OR GRANT NUMBER(s)  F04701-83-C-0084
11. CONTROLLING OFFICE NAME AND ADDRESS Space Division Los Angeles Air Force Station Los Angeles, Calif. 90009		10. PROGRAM ELEMENT, PROJECT, TASK AREA & WORK UNIT NUMBERS
14. MONITORING AGENCY NAME & ADDRESS (if different from Controlling Office)		12. REPORT DATE 28 January 1985
		13. NUMBER OF PAGES 31
		15. SECURITY CLASS. (of this report)  Unclassified
		15a. DECLASSIFICATION/DOWNGRADING SCHEDULE
16. DISTRIBUTION STATEMENT (of this Report)  Approved for public release; distribution unlimited.		
17. DISTRIBUTION STATEMENT (of the abstract entered in Block 20, if different from Report)		
18. SUPPLEMENTARY NOTES		
19. KEY WORDS (Continue on reverse side if necessary and identify by block number) Absorptance Calorimeter Emittance High temperature Laser		
20. ABSTRACT (Continue on reverse side if necessary and identify by block number) A differential calorimeter designed to measure total hemispherical emittance and normal spectral absorptance as a function of temperature is described. The mathematical analysis necessary to calculate both of these parameters is presented. The experimental results obtained with a sample of SiC/Al <sub>2</sub> O <sub>3</sub> (silicon carbide/alumina) are discussed. It was found that the emittance of SiC/Al <sub>2</sub> O <sub>3</sub> is 1 at 200°C and decreases to about 0.81 at 700°C. The absorptance of CO <sub>2</sub> CW laser radiation (10.6 μm) is 0.85 and remains constant within the range of 600 to 700°C.		

DD FORM 1473  
(FACSIMILE)

UNCLASSIFIED

SECURITY CLASSIFICATION OF THIS PAGE (When Data Entered)

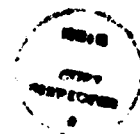
# ACKNOWLEDGMENT

The authors wish to acknowledge the help and encouragement received from Mr. Thomas A. Park throughout the length of this project.

# CONTENTS

ACKNOWLEDGMENT.....	1
I. INTRODUCTION.....	5
II. APPARATUS AND CONTROLS.....	7
III. THEORY OF OPERATION.....	11
IV. CHOICE OF TEST MATERIAL AND EXPERIMENTAL SETUP.....	19
V. RESULTS.....	21
VI. DISCUSSION OF ERRORS.....	25
VII. CONCLUSIONS.....	27
REFERENCES.....	29
APPENDIX: CALCULATION OF VIEW FACTORS.....	31

SEARCHED	<input checked="" type="checkbox"/>
SERIALIZED	<input type="checkbox"/>
INDEXED	<input type="checkbox"/>
FILED	<input type="checkbox"/>
MAR 1964	
FBI - NEW YORK	
A-1	



## FIGURES

1.	Schematic Diagram of Calorimeter.....	8
2.	Assembled Calorimeter.....	9
3.	Expected Behavior of Power Controllers' Output.....	16
4.	Actual Behavior of Power Controllers' Output while Sample A is being Illuminated by the Laser.....	23

## TABLES

1.	Emittance of $\text{SiC}/\text{Al}_2\text{O}_3$ as a Function of Temperature for Samples A and B.....	22
2.	Absorptance of $\text{SiC}/\text{Al}_2\text{O}_3$ at $10.6 \mu\text{m}$ .....	22

## I. INTRODUCTION

This report describes a differential calorimeter designed to measure total hemispherical emittance and normal spectral absorptance of engineering materials over the temperature range 200 to 700°C. This apparatus is of interest because it provides a convenient means for measuring the thermo-optical properties of materials that are degraded by the effects of temperature. In particular, the response of material samples that have been exposed to laser radiation may be significantly affected by changes in the surface optical properties of those samples during exposure.

The thermo-optical properties of engineering materials are generally not available. This is particularly true for properties at elevated temperatures, or for thermally degraded materials. Furthermore, such properties are affected by handling and other environmental or processing conditions to such an extent that direct measurements taken on the specific materials of interest are often the only means of obtaining the data with which one may confidently model material response to thermal-radiation inputs.

The methods for evaluating the emittance and absorptance of materials fall into two general categories: radiometric and calorimetric. Radiometric techniques usually require elaborate equipment and, while capable of relatively high precision, are operational only within the band gap of their detector's sensitivity. Measurements are, for the most part, angle dependent and subject to systematic errors that may be difficult to evaluate. On the other hand, calorimetric techniques are relatively simple and free from systematic errors.<sup>1</sup> Historically, methods for monitoring power and temperature have been crude and of low precision and have made this approach less desirable. Today's electronic devices, however, allow for greater accuracy in measurement. For this work, a calorimetric approach was chosen.

This report discusses the design and operation of a high-temperature (200-700°C) calorimeter. It presents the mathematical analysis necessary to calculate the total hemispherical emittance  $\epsilon(2\pi, T)$  and normal spectral absorptance  $\alpha(\lambda, T)$  of selected materials. This analysis will be applied to experimental data, and the emittance and absorptance at 10.6  $\mu\text{m}$  of  $\text{SiC}/\text{Al}_2\text{O}_3$  as a function of temperature will be calculated. This apparatus provides a novel approach for measuring the laser absorption of materials as a function of temperature and wavelength.

In principle, with a calorimetric technique the emittance or the absorptance of materials may be calculated for either a steady or dynamic state. However, because emittance and absorptance are generally temperature dependent, it is more appropriate to take measurements at equilibrium points. For the approach discussed here, a sample and its surrounding environment are brought to a predetermined temperature. By accounting for all the power inputs as well as the power outputs when a steady-state condition is achieved, one can calculate values for total hemispherical emittance or laser absorptance.

## II. APPARATUS AND CONTROLS

The high-temperature calorimeter designed for this experiment is shown in Figure 1. It is symmetrical through a cross-sectional midplane. Sample materials are positioned in either side of a housing that provides a high-temperature environment. The housing itself, made of oxygen-free, high-conductivity (OFHC) copper, consists of a main body, two sample-carrier rings, and two front plates. Sample assemblies are supported within the carrier rings by means of low-conductivity ceramic standoffs. Each front plate has a circular opening that tapers to a knife edge to minimize the extent to which the plate obscures the sample's view.

To insure that transient thermal deformations do not result in undesirable contact, a gap of about 0.050 in. separates the sample from the knife edge. Each sample is mounted against an OFHC copper block in which two cartridge heaters are imbedded. The main housing is heated separately by a clamshell-type heater. The assembled calorimeter is encased in a gold-coated stainless-steel jacket. Each of the three units (the housing and two samples) has its own temperature controller and power controller. Power transducers monitor the output of the power controllers and provide proportional voltage signals that can be recorded. Twenty thermocouples monitor temperatures throughout the apparatus (see Fig. 2). All electronic devices have been assembled and hardwired into a single console.

A dual calorimeter design was chosen. By testing two samples one can obtain an immediate corroboration of the results: two data points are taken simultaneously. A dual design provides a convenient way for measuring the thermo-optical properties of materials that are degraded by exposure to laser radiation, since electrical power to one of the samples can be monitored continuously while the laser illuminates the other. If, when one measures absorptance the illuminated sample degrades while the other does not, then the degradation is due to the absorptance of the sample at the particular wavelength of the laser being used.

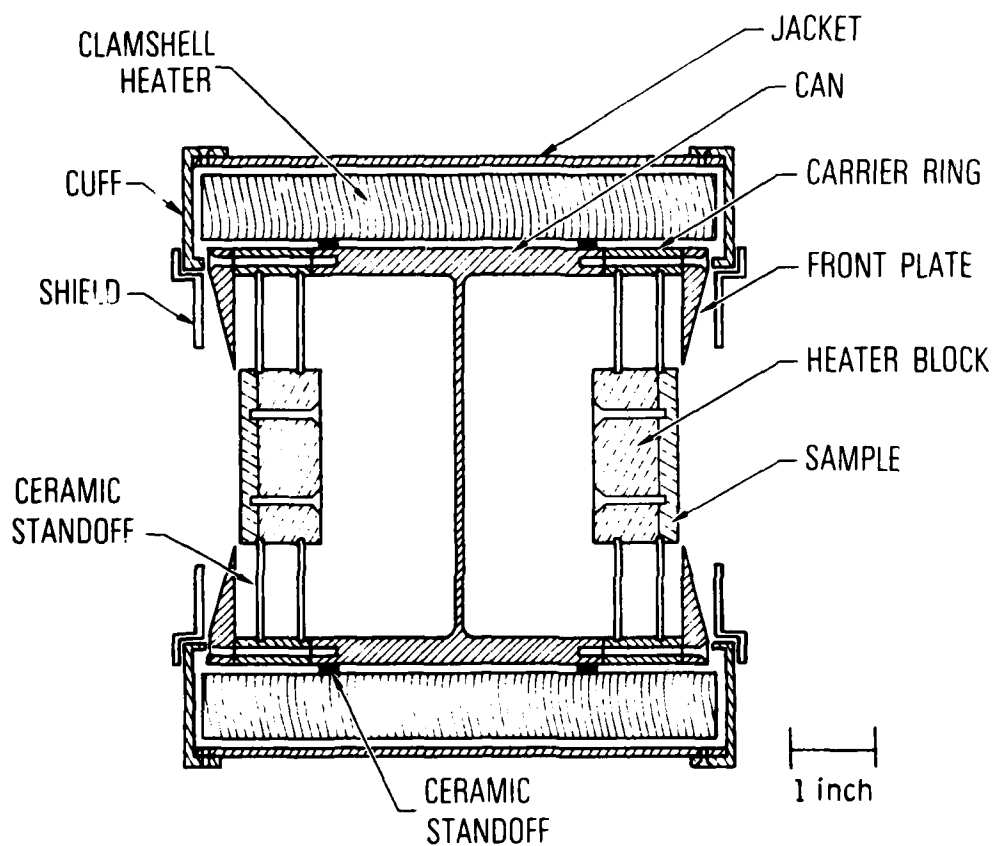


**Fig. 1. Schematic Diagram of Calorimeter.** Calorimeter housing consists of can, carrier ring, and front plate.

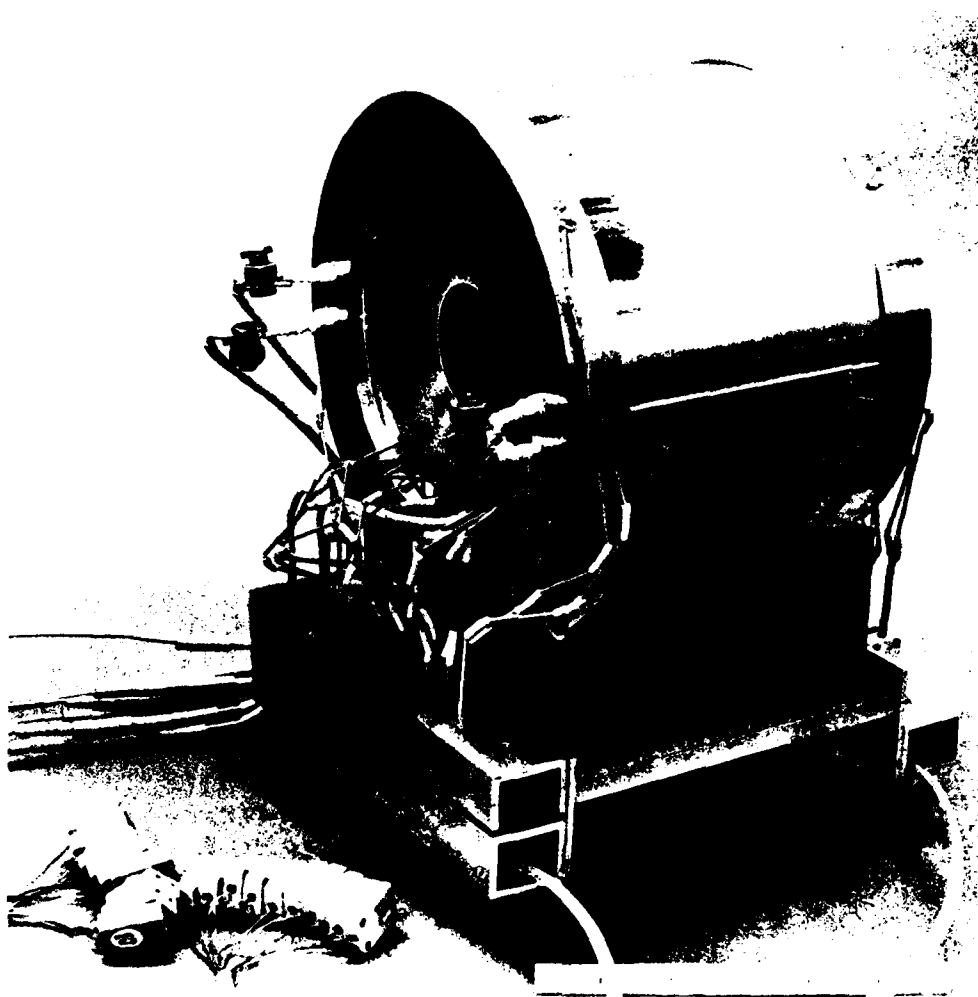


Fig. 2. Assembled Calorimeter (shield not shown)

The operating range of the calorimeter is limited by the failure temperature of the cartridge heaters, which is between 750 and 800°C. To allow for overshooting, 700°C is the maximum temperature for taking data. The minimum allowable temperature is dictated by the temperature controllers, which begin regulating at 200°C.

### III. THEORY OF OPERATION

The temperatures of each of the two samples and the housing of the calorimeter are controlled independently. When a steady-state condition is achieved, i.e., when the housing and samples are the same constant temperature, the power input can be equated to the power output. The task is to account for all the power lost or gained by the sample. Therefore

$$P_{elec} = P_{rad} + P_{cond} + P_{exch} + P_{fg} + P_{cal} \quad (1)$$

where

$P_{elec}$  = total electric power (as measured by the power transducers) needed to keep the sample at a specified temperature

$P_{rad}$  = power radiated by the surface being measured to its surroundings

$P_{cond}$  = power conducted through the standoffs (due to small temperature differences between the sample heating block assembly and the carrier ring)

$P_{exch}$  = power exchanged between the inside surfaces of the housing and the back surfaces of the sample heating block assembly

$P_{fg}$  = fraction of the power (which originates at the sample heating block assembly) radiated by the gap between the sample and front plate

$P_{cal}$  = power discrepancies (due to resistance losses and/or meter calibration) between the transducer reading and actual power

$P_{rad}$  is calculated as follows. According to the Stefan-Boltzmann Law and under the assumption that there are no reflections, the net power radiated by surface 1 in the presence of nearby surface 2 is

$$P = \sigma \epsilon_1 F_{1,2} A_1 T_1^4 - \alpha_1 (\sigma \epsilon_2 F_{2,1} A_2 T_2^4)$$

where

- $\sigma$  = Stefan-Boltzmann constant
- $A_1$  = area of surface 1
- $A_2$  = area of surface 2
- $\epsilon_1$  = emittance of surface 1
- $\epsilon_2$  = emittance of surface 2
- $T_1$  = temperature of surface 1
- $T_2$  = temperature of surface 2
- $F_{1,2}$  = fraction of total surface seen by surface 1 belonging to surface 2. Also called the view factor 1,2
- $F_{2,1}$  = fraction of total surface seen by surface 2 belonging to surface 1. Also called the view factor 2,1
- $\alpha_1$  = absorptance of surface 1

Using Kirchhoff's law,  $\epsilon_1 = \alpha_1$ , and using the fact that for any two surfaces

$$F_{1,2}A_1 = F_{2,1}A_2$$

the power exchanged between the sample and any other surface seen by the sample is

$$P_{\text{rad}} = \sigma \epsilon_1 A_1 \sum_{j=2}^n F_{1,j} (T_1^4 - \epsilon_j T_j^4) \quad (2)$$

where the subscript 1 refers to the sample and the running subscript j refers to the surfaces seen by the sample. If the emittances of all the surfaces except that of the sample are known, all the parameters shown are measurable and  $\epsilon_1$  may be calculated. The determination of the view factors is achieved by taking advantage of the axial symmetry of the various apertures in the field of view of the sample. For the calculation of view factors see the Appendix.

The power conducted through eight standoffs holding the sample is calculated from the equation<sup>2</sup>

$$P_{\text{cond}} = 8KA(T_1 - T_{\text{cr}})/l$$

where

- K = thermal conductivity of the ceramic standoffs at the average temperature of the housing
- A = cross-sectional area of a standoff
- l = length of a standoff
- T<sub>1</sub> = temperature of the sample
- T<sub>cr</sub> = temperature of the carrier ring

The power exchanged between the inner surfaces of the calorimeter and the sample heating block is calculated from the equation

$$P_{\text{exch}} = \frac{\epsilon_{\text{cu}} A_1 \sigma (T_1^4 - T_{\text{av}}^4)}{1 + \frac{A_1}{A_2} (1 - \epsilon_{\text{cu}})}$$

where

- $\epsilon_{\text{cu}}$  = emittance of OFHC polished copper
- $\sigma$  = Stefan-Boltzmann constant
- A<sub>1</sub> = total inner surface area of the calorimeter
- A<sub>2</sub> = total surface area of the sample heating block assembly exposed to the interior cavity of the calorimeter
- T<sub>1</sub> = temperature of sample
- T<sub>av</sub> = average temperature of the housing

Although this equation is developed in Ref. 3 for two concentric cylinders, where edge effects have been ignored (i.e., for cylinders assumed to be of infinite length), it may be used here because the sample assembly surface

exposed to the interior cavity is completely enclosed by the inner surface of the housing. In this case the view factor  $F_{1,2}$  is 1. (In fact, the same equation applies to two concentric spheres.)

The temperature of the housing is not uniform, a problem that becomes more pronounced as the temperature is increased. Each side has three main sections and, although the temperature within these sections remains reasonably constant, the temperature between them differs slightly. For example, when the calorimeter is operated at a temperature of 700°C, there is a temperature difference of about 7°C from the midsection to the front plates. An effective temperature of the housing may be calculated by using a surface-area-weighted average, as follows:

$$T_{av} = \frac{\sum_{i=1}^3 A_i T_i}{\sum_{i=1}^3 A_i}$$

where  $A_i$  is the interior area of a section and  $T_i$  is the corresponding temperature (assumed to be constant within that section).

The power radiated by the gap between the sample and the front plate was calculated by using an emittance of 1 (i.e., the gap was considered to be a blackbody cavity). As this power originates on the surfaces of the interior walls, a ratio of the back surface area of the sample heating block assembly to that of the total interior surface area must be proportional to the ratio of the power originating from the sample heaters to that of the total power radiated by the gap. Therefore

$$P_{fg} = \frac{A_{sb}}{A_t} P_{gap}$$

where

- $P_{fg}$  = fraction of power, emitted through the gap, that originates at the sample heating block assembly
- $A_{sb}$  = area of the sample heating block assembly
- $A_t$  = total area where radiation originates
- $P_{gap}$  = total power radiated by the gap

$P_{gap}$  is computed by using the same equation as for  $P_{rad}$ , Eq. (2), with the corresponding areas and view factors.

Finally,  $P_{cal}$  was determined by evaluating the difference between the output of the power transducer and the output of a calibrated source for the same resistive load. Purely resistive losses in leads were estimated to be negligible.

If  $P_{net}$  is the algebraic sum of  $P_{elec}$ ,  $P_{cond}$ ,  $P_{exch}$ ,  $P_{fg}$ , and  $P_{cal}$ , then, substituting in Eq. (1)

$$P_{net} = P_{rad}$$

Substituting for  $P_{rad}$  from Eq. (2), the total hemispherical emittance  $\epsilon_1$  is

$$\epsilon_1(2\pi, T) = \frac{P_{net}}{\sigma A_1 \sum_{j=2}^n F_{1j} (T_1^4 - \epsilon_j T_j^4)} \quad (3)$$

Laser absorptance as a function of temperature and wavelength may be determined, as with emittance, by first raising the housing and the two samples to the specified temperature with electrical power. Once steady state has been achieved, the front sample is illuminated with a laser (see Fig. 3). The temperature controllers immediately reduce electrical power to the sample. When a new equilibrium is reestablished, at the same temperature as before, the absorptance of the material as a function of temperature and laser wavelength can be extracted from the equation

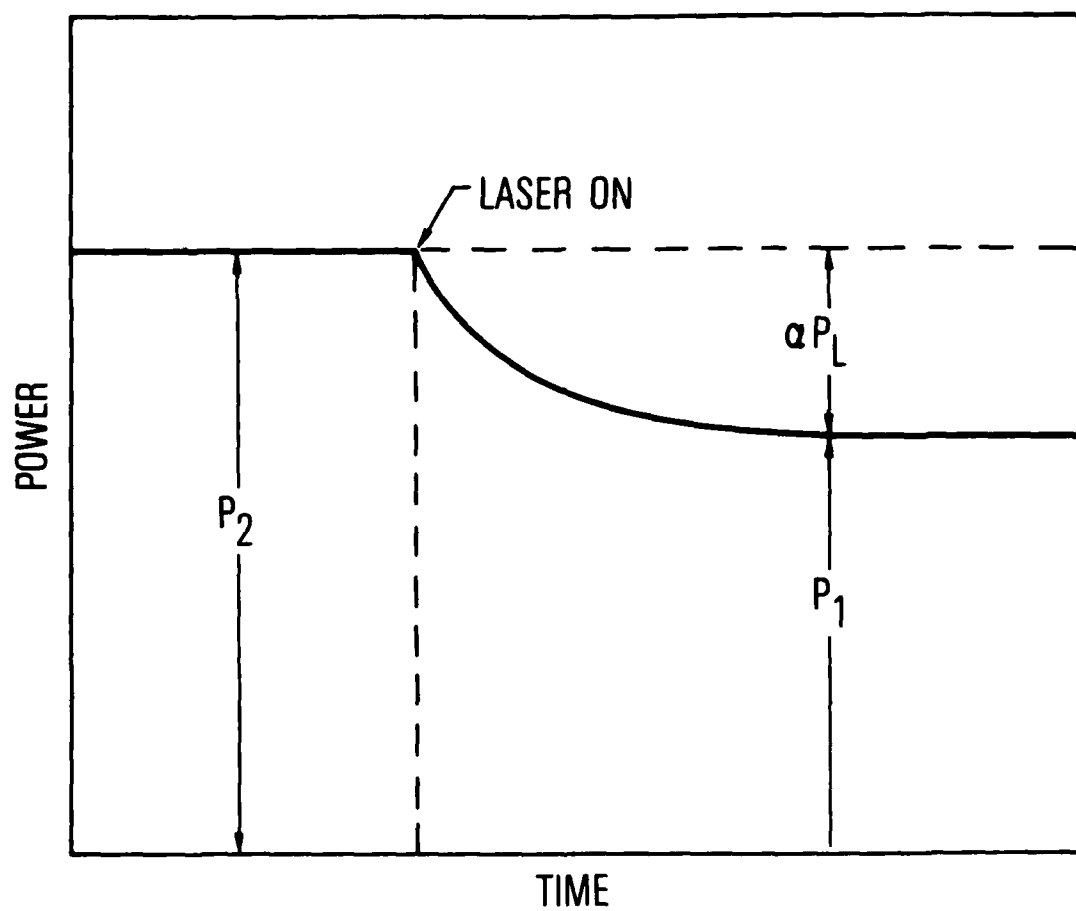


Fig. 3. Expected Behavior of Power Controllers' Output

$$P_2 = P_1 + \alpha P_L$$

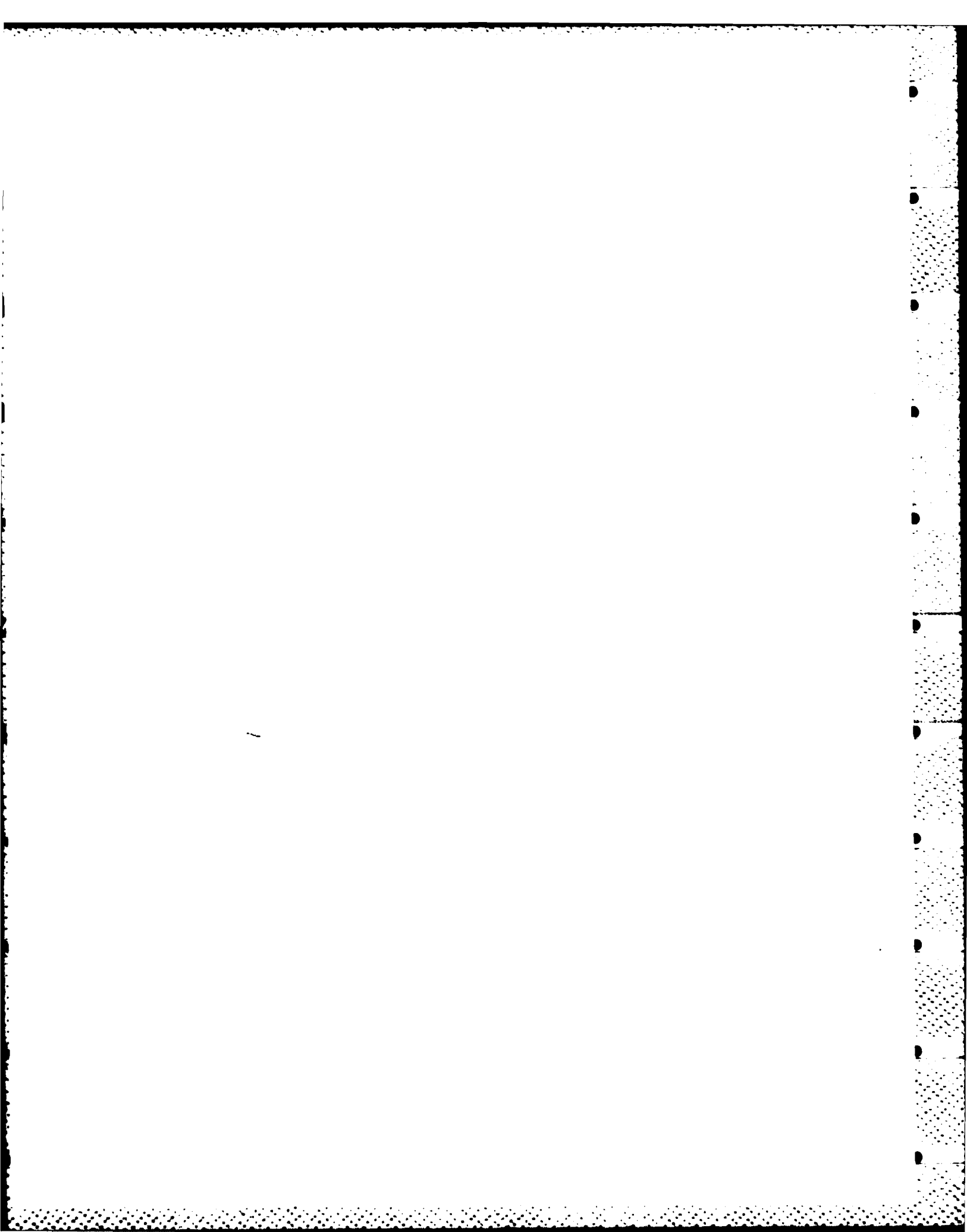
where

- $P_2$  = electrical power at equilibrium before laser is turned on
- $P_1$  = electrical power at the new equilibrium while the laser is illuminating the sample
- $\alpha$  = absorptance of the sample
- $P_L$  = laser power of the laser incident on the sample

Therefore

$$\alpha(\lambda, T) = \frac{P_2 - P_1}{P_L} \quad (4)$$

This approach for measuring the absorptance of a material under laser radiation is particularly attractive. At equilibrium the temperature of the sample is the same before and after the laser is turned on. Therefore, the same experimental conditions exist. Any errors introduced by the view factors and uncertainties in the numerical values of the emittances and temperatures of the obscuring surfaces in the field of view of the sample automatically cancel each other out. The error in measuring the absorptance reduces exclusively to the error introduced in measuring the electrical and laser power.



#### IV. CHOICE OF TEST MATERIAL AND EXPERIMENTAL SETUP

Measurements were made on a  $\text{SiC}/\text{Al}_2\text{O}_3$  coating with a molybdenum substrate.  $\text{SiC}/\text{Al}_2\text{O}_3$  was chosen because of both its apparent stability during temperature cycling and its suspected high emissivity. A molybdenum substrate was selected because molybdenum is a refractory metal and has a coefficient of thermal expansion similar to that of  $\text{SiC}/\text{Al}_2\text{O}_3$ . These characteristics were important for evaluating the overall performance of the calorimeter and establishing its accuracy and operational range. The coating bonded well to the molybdenum substrate and was resistant to thermal shock. Debonding did not occur with repeated cycling between 200 and 700°C. Although the sample darkened slightly after the first cycling to 700°C, no further change was noticed.

Molybdenum disks 2 in. in diameter and 0.25 in. thick were prepared for coating. Blind mounting holes were drilled and tapped on one side and both sides were cleaned and polished. A coating 0.013 to 0.015 in. thick was flame-sprayed from a  $\text{SiC}/\text{Al}_2\text{O}_3$  powder (in the ratio of 25% SiC to 75%  $\text{Al}_2\text{O}_3$ ) onto the untapped sides. The disks were anchored with screws to the heating blocks and then were assembled into the calorimeter. Care was taken to ensure that good thermal contact was made between the samples and heating block surfaces. Two thermocouples were embedded in grooves at these junctions.

The assembled calorimeter was placed in a vacuum chamber with a liquid-nitrogen-cooled shroud. Operational pressures were below 100 mTorr for low temperature (200°C) and increased as high as 200 mTorr at high temperature (700°C).

## V. RESULTS

Data were taken at 100°C intervals in the range of 200 to 700°C. Values for the total hemispherical emittance were calculated by using Eq. (3). These results are presented in Table 1. It was found that for SiC/Al<sub>2</sub>O<sub>3</sub> the emittance was 1 at 198°C and that it decreased to about 0.81 at 692°C.

Initially there was an unexpected problem in taking absorptance data. It was anticipated that laser power would replace electric power and that the temperature of the laser-illuminated sample would remain constant. In actual practice, this did not happen. During the limited laser exposure period, laser power did indeed replace electric power, but the sample stabilized at a temperature several degrees higher than the housing. To overcome this, it was necessary to begin laser illumination with the sample at a temperature a few degrees lower than the housing. This procedure yielded excellent results.

Measurements for laser absorptance were made at 600 and 700°C for several levels of laser flux. Values for the absorptance were obtained by using Eq. (4). These results are presented in Table 2. An actual absorptance curve is shown in Fig. 4.

The temperature controllers, although very consistent in achieving repeatable values, were not accurate in reaching target temperatures. For expediency in cases in which equilibrium was achieved at a temperature slightly different from the target temperature, data were taken at the equilibrium point.

Table 1. Emittance of SiC/Al<sub>2</sub>O<sub>3</sub> as a Function of Temperature for Samples A and B.

Temperature, $\pm 1^\circ\text{C}$	Emittance	
	Sample A	Sample B
692	$0.82 \pm 0.04$	$0.81 \pm 0.04$
596	$0.83 \pm 0.04$	$0.84 \pm 0.04$
497	$0.86 \pm 0.04$	$0.86 \pm 0.04$
398	$0.87 \pm 0.04$	$0.88 \pm 0.04$
300	$0.95 \pm 0.05$	$0.94 \pm 0.05$
198	$1.01 \pm 0.05$	$1.00 \pm 0.05$

Table 2. Absorptance of SiC/Al<sub>2</sub>O<sub>3</sub> at 10.6  $\mu\text{m}$  \*

Run No.	$P_2 - P_1$	$P_L, \pm 2 \text{ W}$	Temperature, $\pm 1^\circ\text{C}$	$\alpha(\lambda, T)$
1	48	57	699	$0.85 \pm 0.03$
2	38	46	699	$0.83 \pm 0.04$
3	33	38	699	$0.87 \pm 0.05$
4	44	51	599	$0.87 \pm 0.04$
5	42	51	599	$0.83 \pm 0.04$
6	37	42	599	$0.88 \pm 0.05$

\* Sample was illuminated with a CO<sub>2</sub> CW laser.

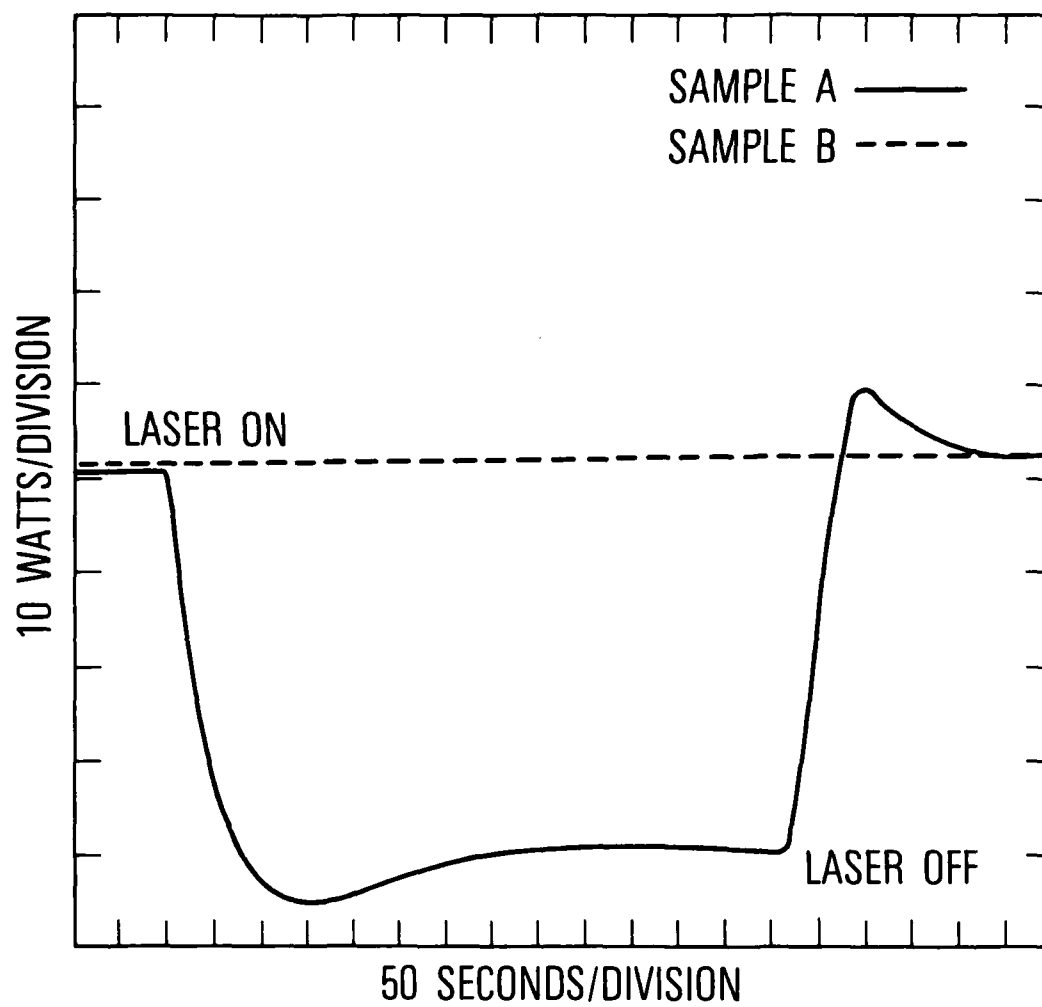


Fig. 4. Actual Behavior of Power Controllers' Output while Sample A is being Illuminated by the Laser

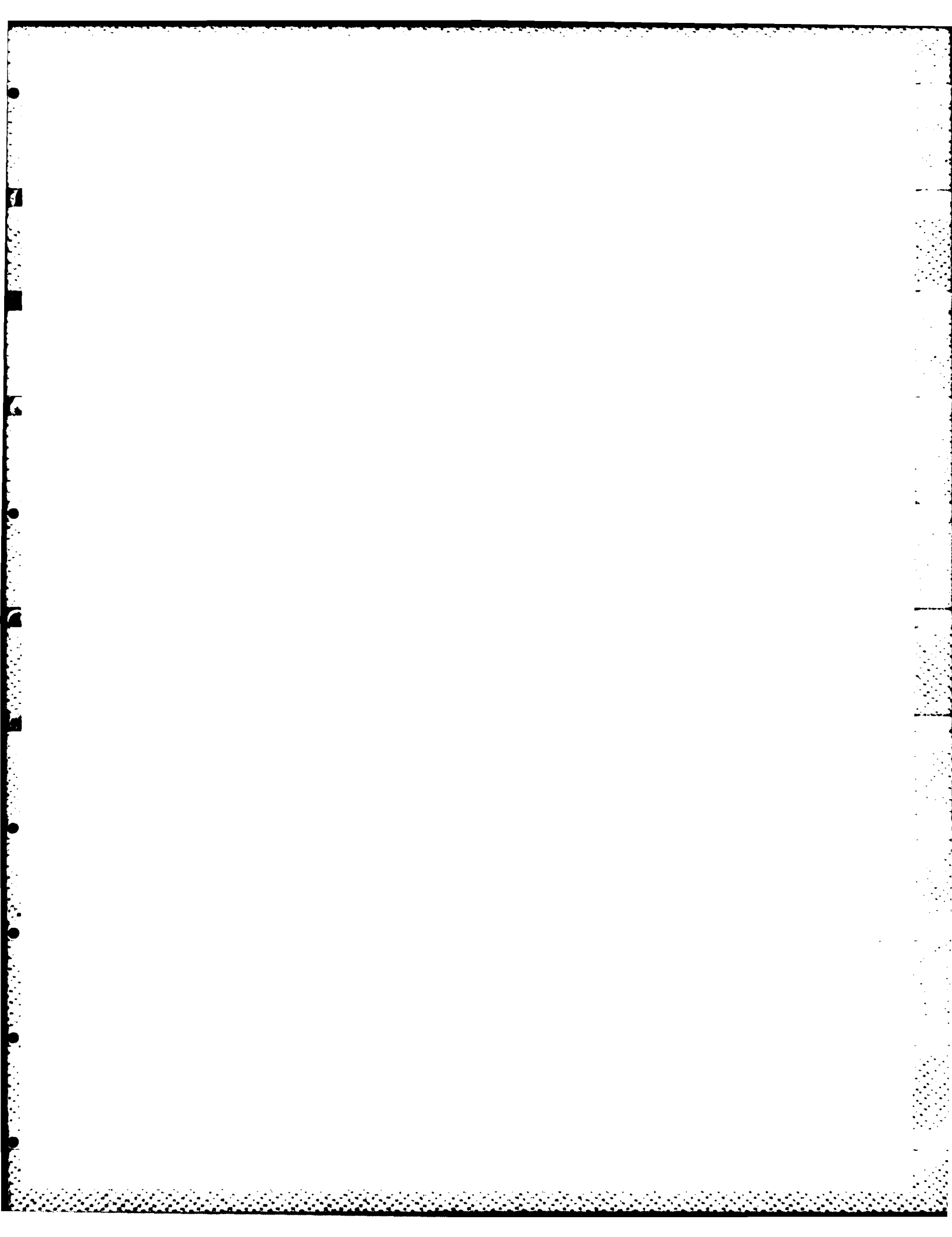
In runs 1 through 3 the laser flux was varied while the temperature was held constant at 699°C. For runs 4 through 6 the laser flux was also varied, but the temperature was 599°C. It was found that the absorptance of SiC/Al<sub>2</sub>O<sub>3</sub> at a CO<sub>2</sub> laser wavelength (10.6 μm) and within the approximate temperature range of 600 to 700°C remains constant within the experimental error at about 0.86. At lower temperatures, a minimum of 30 W or less of laser power was needed to evaluate the absorptance. At such low levels of output, for the setup used in this experiment, the laser was unstable and measurements were not possible.

## VI. DISCUSSION OF ERRORS

For measures of both the emittance and absorptance, the major source of error is in determining values for the electrical power that heats the sample. The error introduced by the measuring instruments,  $\pm 0.5\%$ , is overshadowed by the effects that temperature differences in the housing have on the amount of power that heats the sample. These effects appear at both ends of the operating range. OFHC copper becomes highly reflective when heated in vacuum. Attempts at decreasing this reflectance with high temperature manifold paints proved unsuccessful. At a temperature of  $200^{\circ}\text{C}$ , the calorimeter takes an excessively long time (usually several hours) to come to equilibrium. At a temperature of  $700^{\circ}\text{C}$ , both of the front plates may be as much as  $7^{\circ}\text{C}$  cooler than the center of the calorimeter. If the temperature is not at equilibrium and uniform, the power readings for the samples are inaccurate, making the error introduced by these temperature differences difficult to address. The uniformity of the temperature of the calorimeter improves if the device is left undisturbed for long periods of time. By recording the changes in power as temperature uniformity improves and by extrapolating, it is possible to estimate this error. A conservative estimate of the error in the power readings resulting from temperature differences is  $\pm 5\%$ . This number is used to compute the error in emittance values.

An additional source of error is the uncertainty in the values of the emittances  $\epsilon_j$  of the surfaces seen by the sample. However, this error is very small and well within the  $\pm 5\%$  uncertainty of the power readings for all except the first two surfaces. The reason for this is that all the surfaces except the gap and the front plate are at temperatures much lower than the sample. Because of the fourth power law, the first term predominates. The emittance for the gap was taken as 1.0 and, for the front plate (cleaned OFHC copper), a moderate 0.1.

For the measurements of laser absorptance, the major source of error was introduced by the difficulties in measuring the laser power. The  $\text{CO}_2$  CW laser used was stable only within  $\pm 2$  W of power delivered to the sample. This number was used to calculate the error.



## VII. CONCLUSIONS

In order to determine the accuracy of the calorimeter for measuring the emittance and absorptance of materials, it would be desirable to compare results obtained with the calorimeter to a standard. Unfortunately, up to the present, efforts to locate a standard have been unsuccessful. It appears that the National Bureau of Standards has discontinued manufacturing calibrated sources for emittance as a function of temperature. As for absorptance as a function of temperature and wavelength, a calibrated source has never been produced.

The values for the emittance and absorptance of SiC/Al<sub>2</sub>O<sub>3</sub> obtained with the calorimeter appear reasonable. The high absorptance of SiC/Al<sub>2</sub>O<sub>3</sub> was substantiated, at least at room temperature. Measurements of the total hemispherical reflectance in the infrared between 2.5 and 20  $\mu$ m with a Fourier transform infrared device gave null results for the same samples before and after testing with the calorimeter.

Although the apparatus described here functions well, several modifications to increase its efficiency are being contemplated. Some are intended to improve temperature uniformity, and others will result in a more rapid sample turnaround time. Preliminary tests indicate that if a base coating with an intermediate coefficient of thermal expansion is used, it may be possible to coat the outer surface of the housing with SiC/Al<sub>2</sub>O<sub>3</sub>. If this approach is successful, the emittance and absorptance of the housing will be increased considerably, and the time to reach equilibrium will be greatly shortened.

The approach for establishing values for the total hemispherical emittance and normal spectral absorptance (under laser irradiation) of engineering materials described in this report shows promise. Some small changes should be made in the apparatus to reduce both temperature difference and the time necessary to reach equilibrium, but data already taken are consistent and repeatable. Testing of the thermo-optical properties of materials other than SiC/Al<sub>2</sub>O<sub>3</sub> will constitute the next phase of this work.

#### REFERENCES

1. Y. S. Touloukian, D. P. DeWitt, and R. S. Hernicz, "Thermal Radiative Properties: Coatings," in Thermophysical Properties of Matter, IFI/Plenum (New York, 1972).
2. H. S. Carslaw and J. C. Jaeger, Conduction of Heat in Solids, Oxford University Press (1959).
3. H. C. Hottel and A. F. Sarofim, Radiative Transfer, McGraw-Hill (1967).

## APPENDIX: CALCULATION OF VIEW FACTORS

In order to calculate view factors, axial symmetry is exploited. For two concentric circular areas the view factor is given by

$$F_{1,2} = \frac{1}{2} (Z - \sqrt{Z^2 - 4X^2Y^2})$$

where

$$X = a/c$$

$$Y = c/b$$

$$Z = 1 + (1 + X^2)Y^2$$

and

a = radius of area 1

b = radius of area 2

c = distance between the two areas

By computing the view factors between the sample and any two concentric circular areas and subtracting one from the other, the view factor between the sample and the wall between the two concentric areas is calculated.

By computing the products  $A_1 F_{1j}$  and  $A_1 F_{1,j+1}$  and subtracting one from the other, the resulting view factor between  $A_1$  and the wall between  $A_j$  and  $A_{j+1}$  is calculated. By repeating the process for  $A_{i+1}$  and subtracting the two results, the view factor between any two walls can be obtained. The only requirement is that the circular areas have a common normal axis through their centers. This method was used to compute the view factors between the gap and all surfaces seen by the gap.

#### LABORATORY OPERATIONS

The Laboratory Operations of The Aerospace Corporation is conducting experimental and theoretical investigations necessary for the evaluation and application of scientific advances to new military space systems. Versatility and flexibility have been developed to a high degree by the laboratory personnel in dealing with the many problems encountered in the nation's rapidly developing space systems. Expertise in the latest scientific developments is vital to the accomplishment of tasks related to these problems. The laboratories that contribute to this research are:

Aerophysics Laboratory: Launch vehicle and reentry fluid mechanics, heat transfer and flight dynamics; chemical and electric propulsion, propellant chemistry, environmental hazards, trace detection; spacecraft structural mechanics, contamination, thermal and structural control; high temperature thermomechanics, gas kinetics and radiation; cw and pulsed laser development including chemical kinetics, spectroscopy, optical resonators, beam control, atmospheric propagation, laser effects and countermeasures.

Chemistry and Physics Laboratory: Atmospheric chemical reactions, atmospheric optics, light scattering, state-specific chemical reactions and radiation transport in rocket plumes, applied laser spectroscopy, laser chemistry, laser optoelectronics, solar cell physics, battery electrochemistry, space vacuum and radiation effects on materials, lubrication and surface phenomena, thermionic emission, photosensitive materials and detectors, atomic frequency standards, and environmental chemistry.

Electronics Research Laboratory: Microelectronics, GaAs low noise and power devices, semiconductor lasers, electromagnetic and optical propagation phenomena, quantum electronics, laser communications, lidar, and electro-optics; communication sciences, applied electronics, semiconductor crystal and device physics, radiometric imaging; millimeter wave, microwave technology, and RF systems research.

Information Sciences Research Office: Program verification, program translation, performance-sensitive system design, distributed architectures for spaceborne computers, fault-tolerant computer systems, artificial intelligence and microelectronics applications.

Materials Sciences Laboratory: Development of new materials: metal matrix composites, polymers, and new forms of carbon; nondestructive evaluation, component failure analysis and reliability; fracture mechanics and stress corrosion; analysis and evaluation of materials at cryogenic and elevated temperatures as well as in space and enemy-induced environments.

Space Sciences Laboratory: Magnetospheric, auroral and cosmic ray physics, wave-particle interactions, magnetospheric plasma waves; atmospheric and ionospheric physics, density and composition of the upper atmosphere, remote sensing using atmospheric radiation; solar physics, infrared astronomy, infrared signature analysis; effects of solar activity, magnetic storms and nuclear explosions on the earth's atmosphere, ionosphere and magnetosphere; effects of electromagnetic and particulate radiations on space systems; space instrumentation.

**END**

**FILMED**

**4-85**

**DTIC**